

# Electron Impact Spectroscopy

SANDOR TRAJMAR

California Institute of Technology, Jet Propulsion Laboratory, Pasadena, California 91103

Received August 16, 1979

The quantum states of atoms and molecules traditionally have been investigated by the methods of optical spectroscopy. In recent decades, however, a number of new techniques have been developed to complement optical ones. Among them electron impact spectroscopy plays a prominent role.

Collision of electrons with isolated atoms and molecules can cause a large variety of processes (excitation, ionization, dissociation, electron capture, etc.). In this Account we are concerned only with processes where the electron collision results in a transfer of kinetic energy into the excitation (or deexcitation) of the target species. Comprehensive reviews on electron impact spectroscopy have been published by Berry,<sup>1</sup> Trajmar et al.,<sup>2</sup> Bonham,<sup>3</sup> Brion,<sup>4</sup> Lassetre,<sup>5</sup> and Celotta and Heubner.<sup>6</sup> For a detailed account on the more general subject of electron collision phenomena the reader is referred to the monographs of Massey and Burhop<sup>7</sup> and to a short discussion by Trajmar.<sup>8</sup>

In electron impact spectroscopy a nearly monoenergetic beam of electrons collides with a gaseous atomic or molecular target. The interaction of the incoming low and intermediate energy electrons is strongest with the valence shell electrons of the molecule and causes the distortion of this shell. The consequence of this distortion is excitation of one or more of the valence electrons and/or the nuclear motion (vibration) of the molecule (which is coupled to the field set up by the electron shell). Excitation of individual electrons and vibrational motion to the continuum lead to ionization and to dissociation, respectively. The energy demand required for these processes and the nature of the interaction are reflected in the energy and angular distribution of the scattered electrons.

Electron impact experiments are conceptually simple: electrons of known energy are scattered by individual atoms or molecules, and the energy and angular distribution of the scattered electrons are measured individually or in coincidence with other secondary species. A schematic representation of the experiment is shown in Figure 1. In actual practice a number of difficulties are encountered in generating the monoenergetic electrons, in detecting and analyzing the scattered electrons, and in designing a scattering geometry which makes both the experiment and the interpretation simple. Various approaches have been tried to overcome these problems.<sup>9-11</sup> We will discuss here only the methods which are most frequently used in present day investigations. More details about the instrumentation can be found in ref 12 and 13.

Electrons are extracted from a thermionic source and

Sandor Trajmar was born in Hungary in 1931 and completed his undergraduate education at the Lajos Kossuth University of Science, Debrecen. His graduate work at the University of California was concerned with high-temperature chemistry and spectroscopy. After receiving his Ph.D. degree in physical chemistry, he joined the California Institute of Technology and held joint appointments at the Jet Propulsion Laboratory and the Division of Chemistry and Chemical Engineering. At the present time, he is the head of the Electron Collision Processes Group at JPL and is involved with low- and intermediate-electron collision phenomena and spectroscopy.

collimated and focused into an energy selector with an electrostatic lens train. For the electron lenses, electrostatic apertures or cylinders are most commonly used. The energy selector is usually a pair of hemispheres or cylinders utilizing electrostatic deflection to spatially separate electrons of different energy. Other types of selectors, like retarding field analyzers, parallel plate analyzers, trochoidal monochromators, and Wien-filter and Möllenstedt analyzers, have also been used with success. Electrons with a narrow energy distribution are then focused with the required impact energy ( $E_0$ ) into the target region. The scattered electrons are collected over a small solid angle ( $\sim 10^{-3}$  sr) at some scattering angle  $\theta$ , and their energy is analyzed with devices similar to those used to achieve the energy selection in the incoming electron beam. Electrons with a specific residual energy  $E_R$  pass through the analyzer and are detected with an electron multiplier which generates a current pulse for each electron. This signal is then recorded as a function of some parameter ( $E_0$ ,  $E_R$ ,  $\theta$ ) utilizing pulse counting and multichannel scaling techniques.

The target may be a static gas contained in a box or, more frequently, an atomic or molecular beam. The beam is generated by effusing the gas through an orifice, a tube, or a capillary array with or without further collimation. Supersonic nozzle beams for high target densities and high-temperature crucible sources for materials which have low vapor pressure at room temperature are also frequently used.

The apparatus is mounted in a vacuum chamber and the background pressure is generally kept below  $10^{-5}$  torr during the measurements. At these pressures the mean free path of an electron is large compared to the size of the target or that of the whole apparatus. It is very important to eliminate the effects of magnetic and electric fields on the electrons. One, therefore, has to use electrostatic and magnetic shields.

The electron impact spectrometer can be operated in

- (1) R. S. Berry, *Annu. Rev. Phys. Chem.*, **20**, 357 (1969).
- (2) S. Trajmar, J. K. Rice, and A. Kuppermann, *Adv. Chem. Phys.*, **18**, 15 (1970).
- (3) R. A. Bonham, "Theory of Electron Impact Spectroscopy of Atoms and Molecules", University Park Press, Baltimore, 1971.
- (4) C. E. Brion, *MTP Int. Rev. Sci.: Phys. Chem. Ser. Five*, **55** (1972).
- (5) E. N. Lassetre in "Chemical Spectroscopy and Photochemistry in the Vacuum Ultraviolet", C. Sandorfy, P. Ausloos, and M. B. Robin, Eds., D. Reidel, Dordrecht-Holland, 1974, pp 43-73.
- (6) R. J. Celotta and R. H. Heubner in "Electron Spectroscopy. Theory, Techniques and Applications", Vol. 3, C. R. Brundle and A. D. Barker, Eds., Academic Press, 1979, pp 41-125.
- (7) H. S. W. Massey and E. H. S. Burhop, "Electronic and Ionic Impact Phenomena", Vol. I, Clarendon Press, Oxford, 1969; H. S. W. Massey, *ibid.*, Vol. II.
- (8) S. Trajmar, *Science*, in press.
- (9) C. E. Kuyatt, *Methods Exp. Phys.*, Part **B**, **7**, 1-89, (1968).
- (10) B. Bederson and L. J. Kieffer, *Rev. Mod. Phys.*, **43**, 601 (1971); D. E. Golden, N. F. Lane, A. Temkin, and E. Gerjuoy, *ibid.*, **43**, 642 (1971).
- (11) R. A. Bonham and M. Fink, "High Energy Electron Scattering", Van Nostrand-Reinhold, 1974; "Electron Spectroscopy: Theory Techniques and Applications", Vol. 3, C. R. Brundle and A. D. Baker, Eds., Academic Press, London, 1979, Chapter 3.
- (12) A. Chutjian, *J. Chem. Phys.*, **61**, 4279 (1974).
- (13) S. Jensen, Ph.D. Thesis, University of California, Riverside, 1978.

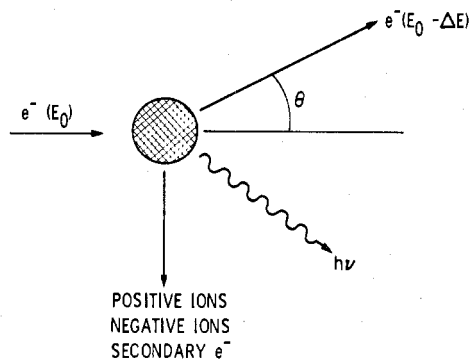


Figure 1. Schematic electron scattering experiment.

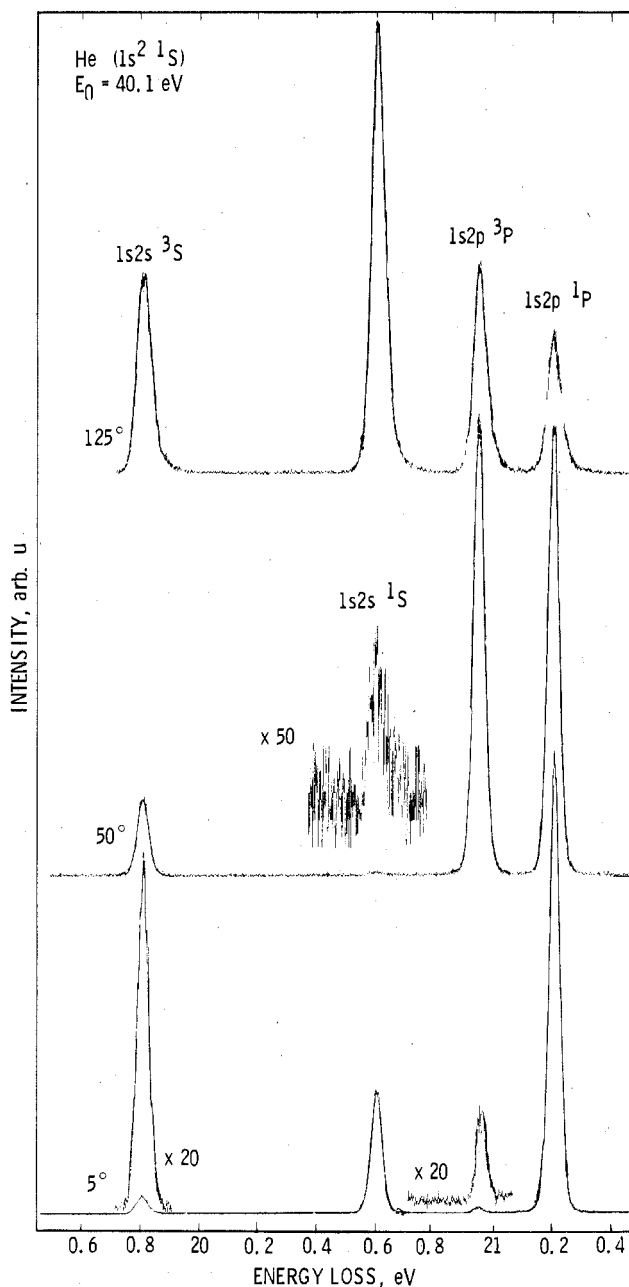


Figure 2. Energy-loss spectrum of He in the 19.6- to 21.4-eV region at 40.1-eV impact energy and 5, 50, and 125° scattering angles.

a number of ways. The most commonly used mode is the energy loss mode. In this case  $E_0$  and  $\theta$  are kept fixed, and the scattered signal intensity is measured as a function of energy lost by the electron ( $\Delta E = E_0 - E_R$ ) during the collision. The zero-energy-loss feature corresponds to elastic scattering, and the other features

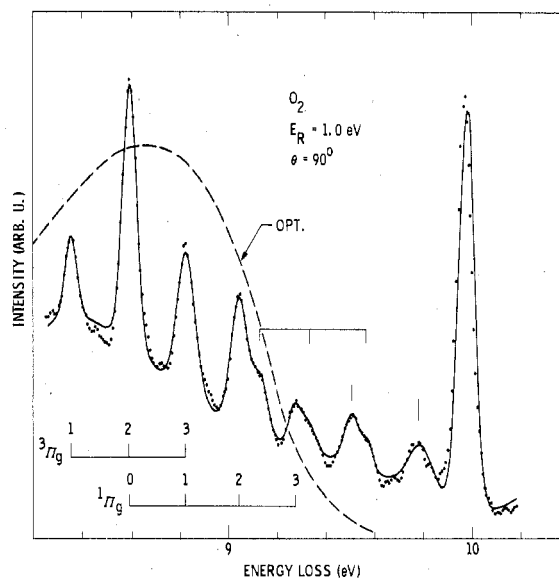


Figure 3. Energy-loss spectrum of  $O_2$ . (See text for explanation.)

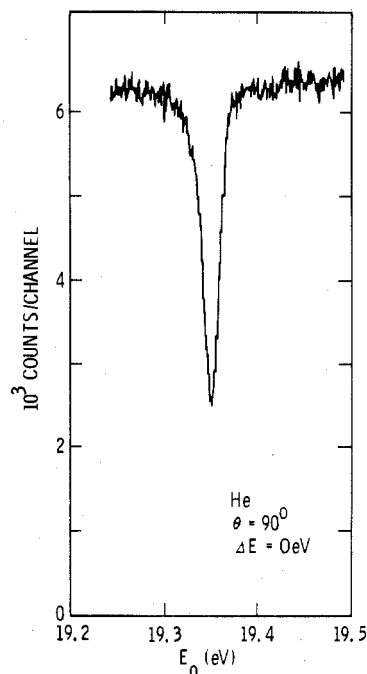


Figure 4. The 19.3-eV resonance of He as observed in the elastic channel at 90° scattering angle.

appearing in the spectrum correspond to various excitation processes. Typical energy-loss spectra are shown in Figure 2.<sup>14</sup> Energy-loss spectra can also be generated in the constant residual energy mode. In this case the analyzer is made to transmit only electrons which have a specific residual energy ( $E_R$ ) after the scattering process. That is, the condition  $E_R = \text{const} = E_0 - \Delta E$  is satisfied during the scanning of the whole spectrum, and each feature or transition is generated at the same energy above its own threshold at a fixed  $\theta$ . This mode of operation is useful at low impact energies where the energy sensitivity of the detector lens system could drastically alter the energy-loss spectrum obtained by the first method of operation. An energy-loss spectrum obtained this way is shown in Figure 3.<sup>15</sup> In the third method of operation the detector is set to transmit only at a specific energy-loss channel ( $\Delta E$  and  $\theta$  fixed), and

(14) S. Trajmar, *Phys. Rev. A*, 8, 191 (1973).

(15) S. Trajmar, D. C. Cartwright and R. I. Hall, *J. Chem. Phys.*, 65, 5275 (1976).

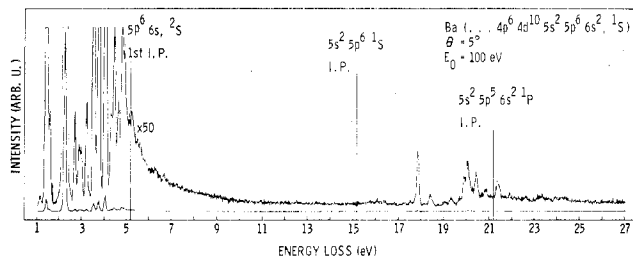


Figure 5. Energy-loss spectrum of Ba. (See text for explanation.)

in this case the electron impact energy is swept to study the energy dependence of a particular excitation process. This method is used to study resonances (associated with electron capture processes) and cusps which appear in various channels. See Figure 4 for an example.<sup>16</sup>

There are many similarities, but also significant differences, between optical and electron impact spectroscopy. The electron impact spectrum of He shown in Figure 2 is very similar to an optical absorption spectrum. The locations of the various spectral features are related to the energy level pattern of the target, and the scattering intensity is related to the probability of the excitation processes. In high-energy electron scattering the target experiences a sharply pulsed (in time) electric field. The frequency components of this field can be obtained from a Fourier transform, and they represent a wide range of frequencies of essentially equal intensity. The high-energy electron therefore represents an ideal continuum light source, and the energy-loss spectrum generated by it resembles an optical absorption spectrum. However, a low-energy electron impact spectrum differs in this respect. In Figure 2 the only optically allowed transition is the excitation from the ground ( $1s^2$ ) $^1S$  to the ( $1s2p$ ) $^1P$  excited state. The other three excitation processes are forbidden by dipole selection rules and have negligible probability in the photoabsorption spectrum. This is certainly not the case in the electron impact spectrum.

There are no general selection rules for electron impact excitations. In addition to the optically allowed transitions, symmetry and/or spin-forbidden excitations occur with high probability. As the scattering conditions change (as demonstrated in Figure 2 by changing the scattering angle), the character of the spectrum changes drastically. At low angles (and high energies) the optically allowed transitions dominate, while at high angles (and low energies) the optically forbidden transitions become comparable to, or stronger than, the optically allowed ones. This behavior of the spectrum can be exploited to reveal energy levels of a target which are not detectable by optical means.

The electron impact spectra can also be considered analogous to Raman spectra. The elastic peak (zero energy loss) corresponds to Rayleigh scattering; the inelastic features correspond to Stokes lines; and the superelastic features (collisions where the electron gains energy from the target) correspond to anti-Stokes lines. The analogy is again not perfect, because Raman selection rules are not generally obeyed either.

A second obvious difference illustrated by Figure 5 is the range of the spectrum which the electron impact technique can cover with the same instrument in a single scan. It extends from the extreme IR (actually

zero frequency) to the X-ray region. Several very different optical techniques are required to achieve the same coverage. Although the resolution of optical techniques in the IR and visible regions is much superior to electron impact techniques ( $\sim 20$  meV), in the extreme UV and X-ray regions the two methods have comparable resolutions, and the electron impact method yields much higher signal intensities.

A third important difference between the two methods is the extra information that can be learned from the angular distribution of the scattered electrons concerning the assignment of the excited states and the nature of the electron-atom (molecule) interaction.<sup>2,17</sup> Electronic excitations which require spin change occur readily in electron impact excitations because of spin exchange between the molecular and scattering electrons. These spin-exchange processes require short-range interactions and result in an isotropic distribution of the scattered electron. Optically allowed electronic excitations, on the other hand, are associated with forward peaking scattered electron distributions. Parity-forbidden transitions, e.g.,  $\Sigma^+ \leftrightarrow \Sigma^-$  transitions, have zero cross sections for forward and backward scattering, and they can be easily recognized by this behavior.

#### Limit Theorem, Selection Rules

As discussed in the previous section, electrons behave like photons in excitation processes when momentum transfer is small during the collision (high impact energy, low scattering angle). The utilization of electrons as pseudophotons thus makes possible the determination of optical absorption or ionization cross sections by electron impact techniques. This is especially important in the extreme UV and X-ray regions where light sources, with the exception of the rather expensive synchrotron, are not readily available. The electron impact apparatus is considered, from this point of view, as the "poor man's synchrotron".

The concept of generalized oscillator strength for electron scattering was introduced by Bethe<sup>18</sup> and recently discussed in detail by Inokuti.<sup>19</sup> It is expressed by eq 1, where  $d\sigma_{on}^B/d\Omega(K)$  is the Born differential

$$f_{on}^G(K) = \frac{\Delta E}{2} \left( \frac{k_0}{k_n} \right) K^2 \left[ \frac{d\sigma_{on}^B(K)}{d\Omega} \right] \quad (1)$$

cross section for excitation of the target from state  $|\psi_0\rangle$  to state  $|\psi_n\rangle$ ,  $k_n$  and  $k_0$  are the magnitudes of the final and initial momentum of the electron,  $K$  is the magnitude of the momentum transfer ( $\vec{K} = \vec{k}_n - \vec{k}_0$ ), and  $f_{on}^G(K)$  is the generalized oscillator strength. For the continuum the differential (with respect to energy loss) quantities  $d\sigma^B/[d\Omega d(\Delta E)]$  and  $df_{on}^G(K)/d(\Delta E)$  have to be used. The cross section is proportional to the square of the transition matrix element, which in the Born approximation is given as eq 2. Here  $\psi_0$  and  $\psi_n$  are the

$$\frac{d\sigma_{on}^B}{d\Omega}(K) \propto \left| \langle \psi_n | e^{i\vec{k}\cdot\vec{r}} | \psi_0 \rangle \right|^2 \quad (2)$$

initial and final state wave functions, and the exponential is the Born operator. It is easy to show by power

(17) F. H. Read and G. L. Whiterod, *Proc. Phys. Soc. (London)*, **82**, 434 (1963).

(18) H. A. Bethe, *Ann. Phys.*, **5**, 325 (1930).

(19) M. Inokuti, *Rev. Mod. Phys.*, **43**, 297 (1971).

(16) R. I. Hall and S. Trajmar, unpublished.

series expansion<sup>20</sup> that in the limit  $K \rightarrow 0$  this leads to eq 3, where  $f_{0n}^{\text{Opt}}$  is the optical  $f$  value.

$$f_{0n}^{\text{G}}(K) \xrightarrow{K \rightarrow 0} f_{0n}^{\text{Opt}} \quad (3)$$

Lassette et al.<sup>21</sup> extended the use of eq 1 to cases when the Born approximation does not hold and introduced the "apparent generalized oscillator strength"  $f_{0n}^{\text{AG}}(K)$  in place of  $f_{0n}^{\text{G}}(K)$ . He was able to show that even in these cases

$$f_{0n}^{\text{AG}}(K) \xrightarrow{K \rightarrow 0} f_{0n}^{\text{Opt}} \quad (4)$$

which is called the "limit theorem". Equation 4 can be considered as equivalent to a selection rule, namely: in the zero momentum transfer limit, optical selection rules apply to electron impact excitation. The problems with the limit theorem, from the practical point of view, are that it represents a nonphysical limit (even for zero scattering angle the momentum transfer for inelastic scattering is different from zero) and that the extrapolation to zero momentum transfer involves some arbitrariness.

Selection rules for electron impact excitations based on group theoretical arguments have been derived and summarized by Cartwright et al.<sup>22</sup> and Goddard et al.<sup>23</sup> For atoms, the selection rule  $S_g \leftrightarrow S_u$  applies in general (if spin-orbit coupling and other relativistic effects are neglected). In addition, zero angle (and 180°) scattering is forbidden if  $L_i + p_i + L_f + p_f$  is odd. Here  $L_i$  and  $L_f$  are the angular momenta and  $p_i$  and  $p_f$  are the parity numbers of the initial and final electronic states of the atom, respectively.

In the case of molecules, selection rules can be derived under two special conditions: (a) rules concerning 0° and 180° scattering for arbitrary orientation of the molecule and (b) rules concerning scattering though any angle but for specific orientations of the molecule. As an example to case a, we mention the selection rule  $\Sigma^- \leftrightarrow \Sigma^+$  for 0° and 180° scattering angle for diatomic molecules. The interesting behavior of the differential cross section for the excitation of the  $b^1\Sigma_g^+$  state of  $\text{O}_2$  (from the  $X^3\Sigma_g^-$  ground state) was observed by Trajmar et al.<sup>24</sup> and led to the derivation of this<sup>22</sup> and other selection rules.<sup>23</sup> A simple symmetry argument can be utilized to show how this rule comes about. The cross section is proportional to the square of the transition matrix element:

$$\frac{d\sigma}{d\Omega} \propto |\langle \Psi_f | T | \Psi_i \rangle|^2 \quad (5)$$

where  $\Psi_i$  and  $\Psi_f$  are the initial and final wave functions for the  $N + 1$  electron system and  $T$  is the transition operator. Although we do not know the exact forms of these functions and the operator, we do know their symmetry properties under the operations of the point group of the electron-molecule system. On the basis of the physics of the scattering,  $T$  is known to be totally

symmetric. In order to get nonvanishing matrix elements in eq 5 (which represents integration from  $-\infty$  to  $+\infty$ ), the product representation  $[\Psi_f \Psi_i]$  also has to be totally symmetric. The  $N + 1$  electron wave function can be factored as

$$\Psi = \psi^e \psi^V \psi^R f_e \quad (6)$$

where  $\psi^e$ ,  $\psi^V$ , and  $\psi^R$  are the electronic, vibrational and rotational wave functions, respectively, and  $f_e$  is the scattered electron wave function. Here the Born-Oppenheimer adiabatic approximation, which has been found to be valid in general for electron impact excitations independent of  $E_0$  and  $\theta$ ,<sup>25</sup> is applied. The vibrational wave functions in eq 5 yield the Franck-Condon factor just as in optical spectroscopy. Neither the Franck-Condon factor nor the rotational wave functions will influence the present symmetry arguments. For 0° or 180° scattering the symmetry behavior of the scattered electron wave function can be visualized to be totally symmetric under the operations of the point group of the diatomic molecule. The question then boils down to the symmetry properties of the product representation  $[\psi_f^e \psi_e^e]$ . The electronic wave functions for the  $\Sigma^+$  and  $\Sigma^-$  molecular states are symmetric and antisymmetric, respectively, with respect to reflection in the plane of the molecule. This results in an antisymmetric behavior of the product representation and, therefore, in zero value for the transition matrix element in eq 5.

### Specific Examples

**Electron Impact Excitation of Ba.** The complex electronic structure of Ba makes this atom ideally suited for demonstrating a variety of electron impact excitation processes.<sup>26</sup> Figure 5 shows an energy-loss spectrum of Ba. Below the first ionization limit the transitions correspond to the excitation of one of the 6s electrons to various  $nl$  orbitals (where  $n$  and  $l$  are the principal and azimuthal quantum numbers, respectively). Singlet-triplet as well as  $\Delta L = 2$  and 3 transitions have been observed. At 5.2 eV, the first ionization limit, one of the 6s electrons becomes free. In the 5.2- to 15.2-eV region the features correspond to simultaneous excitation of both 6s electrons. At 15.2 eV both of these electrons are excited into the continuum producing  $\text{Ba}^{2+}$  in its ground states. Above this limit the 5p electron excitation (or simultaneous 6s5p excitation) processes appear. At 21.2 eV is the 5p ionization limit, and from here on excitations of the 5s electron (and/or simultaneous excitations of 5s, 6s, 5p electrons) are possible. At still higher energy losses, at around 100 eV (with higher impact energies), the 4d shell excitation can be detected. Above 5.2 eV the excitation features have, in general, resonance shapes because of the interference of the discrete excitations with the underlying continua.

**Rotational Excitation.** Hydrogen is the only molecule for which the rotational excitation structure can be resolved with present day electron-scattering techniques. Pure rotational excitation of homonuclear molecules is optically forbidden but readily occurs with

(20) E. N. Lassette, *J. Chem. Phys.*, **43**, 4479 (1965).

(21) E. N. Lassette, A. Skerbele, and M. A. Dillon, *J. Chem. Phys.*, **50**, 1829 (1969).

(22) D. C. Cartwright, S. Trajmar, W. Williams, and D. L. Huestis, *Phys. Rev. Lett.*, **27**, 704 (1971).

(23) W. A. Goddard, D. L. Huestis, D. C. Cartwright, and S. Trajmar, *Chem. Phys. Lett.*, **11**, 329 (1971).

(24) S. Trajmar, D. C. Cartwright, and W. Williams, *Phys. Rev. A*, **4**, 1482 (1971).

(25) A. Kuppermann, J. K. Rice, and S. Trajmar, *J. Phys. Chem.*, **72**, 3894 (1968).

(26) S. Trajmar, "The Physics of Electronic and Atomic Collisions, Invited Lectures, Review Papers, and Program Reports of the IXth International Conference on the Physics of Electronic and Atomic Collisions", G. Watel, Ed., North-Holland, 1978.

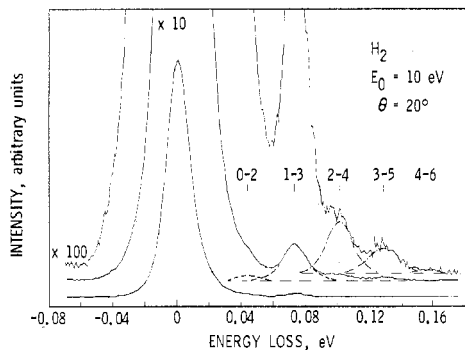


**Figure 6.** Rotational excitation spectrum of  $\text{H}_2$ . The  $J'' - J'$  values for the various excitations are indicated.

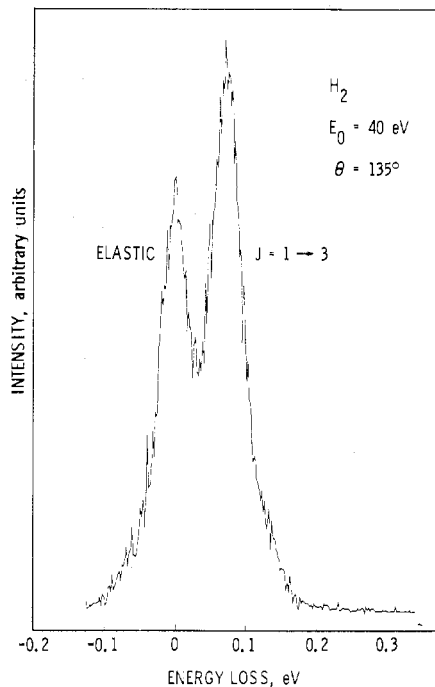


**Figure 7.** Rotational excitation spectrum of  $\text{H}_2$  at high impact energy and scattering angle.

low energy electrons. Rotational excitation ( $\Delta J = 0, 2, 4$ ) have high cross sections at low energies where resonance mechanisms dominate,<sup>27</sup> but even at intermediate energies this process has a significant probability contrary to simple intuition. Energy-loss spectra are shown in Figures 6 and 7.<sup>28</sup> Rotational transitions from  $J > 0$  or 1 levels, which are populated to some extent at room temperature, are also clearly seen at low angles. At higher scattering angles rotational excitation is more important than elastic scattering ( $J$  is the rotational quantum number).

The extreme case for rotational excitation occurs in connection with highly polar molecules where the  $\Delta J = \pm 1$  rotational transition has the highest probability among all the excitation processes.<sup>29</sup> This is due to the long range nature of the dipole interaction.

**Vibrational Excitation.** Electrons are also very effective in exciting molecular vibrations, especially at low impact energies where resonances dominate the cross sections.<sup>30</sup> An example is shown in Figure 8 for

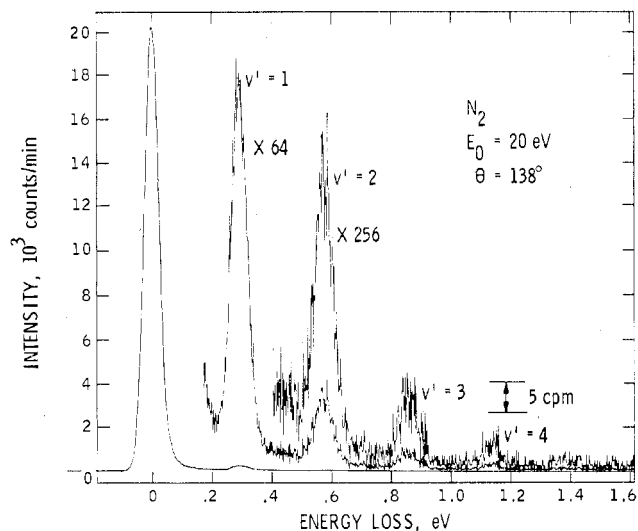


**Figure 8.** Vibrational excitation of  $\text{N}_2$ .

$\text{N}_2$ .<sup>31</sup> The fundamental mode as well as several overtone excitations (all of them optically forbidden) are observed. The probability of exciting the successive overtones decreases by about a factor of 10. The sensitivity of the electron impact method is well demonstrated in this spectrum. The vertical bar in the figure indicates the scattering signal associated with the detection of five electrons per minute. It is evident that signals as low as a few electrons per minute can be detected.

The spectroscopic information obtained from vibrational excitation studies is small compared to optical methods except in the case of optically forbidden excitations and resonance excitations where transitions to high vibrational states can be observed. The reason for this is the modification of the Franck-Condon factors by an intermediate resonant state. Even more extreme cases of high vibrational excitations can be found when the resonant state is a dissociative one. Excitations well above  $v'' = 20$  have been observed for a number of molecules by Greteau et al.<sup>32</sup>

In the case of polyatomic molecules there is an appreciable probability for excitation of numerous overtone and combination bands.

**Electronic Excitation.** The change of an energy-loss spectrum with scattering angle and impact energy has been exploited to reveal electronic energy levels of molecules which are not observable by optical methods. In a recent study of  $\text{O}_2$ , new electronic states have been found by Trajmar et al.<sup>15</sup> under the very strong Schuman-Runge continuum. Figure 3 shows energy-loss spectra of  $\text{O}_2$  in the 8.2 to 10.2 eV energy-loss region. High energy electrons at low scattering angles generate a spectrum which is identical to an optical absorption spectrum (indicated as OPT in the figure). This spectrum is dominated by the Schuman-Runge continuum. As the scattering conditions are changed to low impact energies and high scattering angles the continuum becomes weak and underlying forbidden transitions become apparent. Figure 3 clearly shows the singlet and triplet  $\Pi_g$  excitations as well as additional, still unassigned transitions. Similar studies have re-

(27) G. Joyez, J. Comer, and F. H. Read, *J. Phys. B*, **6**, 2427 (1973).

(28) S. K. Srivastava, R. I. Hall, S. Trajmar, and A. Chutjian, *Phys. Rev. A*, **12**, 1399 (1975).

(29) L. A. Collins and D. W. Norcross, *Phys. Rev. A*, **18**, 467 (1978).

(30) G. J. Schulz, *Rev. Mod. Phys.*, **45**, 423 (1973).

(31) A. Chutjian and S. Trajmar, unpublished.

(32) F. Greteau, R. I. Hall, J. Mazeau, and D. Vichon, *J. Phys. B*, **10**, L545 (1977).

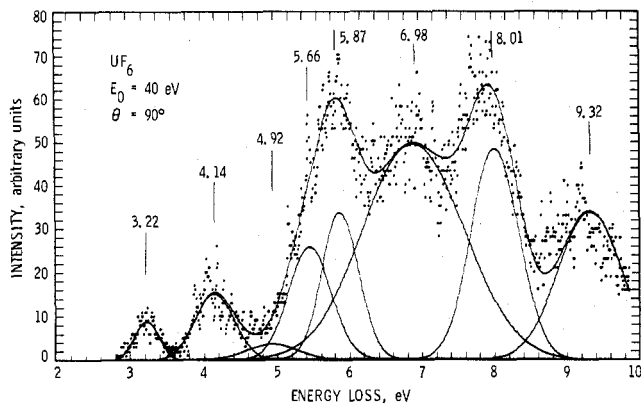


**Figure 9.** Energy-loss spectrum of  $\text{UF}_6$  in the 2- to 10-eV region (dots). The spectrum is decomposed into eight transitions. (See text for explanations.)

vealed new electronic states, e.g., of  $\text{N}_2$ ,<sup>33</sup>  $\text{C}_2\text{H}_2$ ,<sup>34,35</sup>  $\text{LiF}$ .<sup>36</sup> A large number of organic compounds have been studied recently by Kuppermann and co-workers to identify low-lying metastable states in these molecules. (See, e.g., ref 37.) Brion and co-workers investigated the spectra of organic compounds at impact energies of about 100 eV and low scattering angles and generated spectra which are equivalent to optical absorption spectra. (See, e.g., ref 38.)

**Electron Impact Excitation and Photoabsorption Spectrum of  $\text{UF}_6$ .** The interpretation of the spectrum of complex molecules like  $\text{UF}_6$  (shown in Figure 9) requires a coordinated approach utilizing both experimental and theoretical methods. Theoretical methods predict the type of excitations one can expect, their approximate energies, and, more accurately, their relative energies. The experiments define the precise values of transition energies and reveal some information about the Franck-Condon factors and about the nature of the states involved in the transitions. With the combination of all this information, it becomes possible to make spectroscopic assignment. For  $\text{UF}_6$  the spectrum is decomposed into eight electronic transitions on the basis of requiring consistency of spectra at all energies and angles with theory.<sup>39</sup> All transitions are of the charge-transfer type corresponding to transfer of an electron from hybrid orbitals to the 5f and 6d orbitals of U, and they all result in dissociation of the molecule. The energy-loss spectra also reveal that the lowest electronic singlet and triplet charge-transfer excitation from a  $t_{1u}$   $\sigma$  orbital centered on the fluorine atoms to the  $a_{2u}$  uranium 5f orbital occur at about 3 eV.

The optical absorption spectrum of  $\text{UF}_6$  was measured from 4200 to 2000 Å, but no information was available beyond this wavelength region. Utilizing high-energy, low-angle, electron-scattering techniques and the limit theorem, Srivastava et al.<sup>40</sup> generated

(33) D. C. Wilden, P. J. Hicks, and J. Comer, *J. Phys. B*, **12**, 1579 (1979).

(34) S. Trajmar, J. K. Rice, S. P. S. Wei, and H. Kuppermann, *Chem. Phys. Lett.*, **1**, 703 (1968).

(35) G. C. King, J. W. McConkey, and F. H. Read, *J. Phys. B*, **10**, L541 (1977).

(36) L. Vuskovic, S. K. Srivastava, and S. Trajmar, *J. Phys. B*, **11**, 1643 (1978).

(37) R. P. Frueholz, W. M. Flicker, O. A. Mosher, and A. Kuppermann, *J. Chem. Phys.*, **70**, 1986, 2003 (1979).

(38) W. C. Tam and C. E. Brion, *J. Electron Spectrosc. Relat. Phenom.*, **3**, 467 (1974); **4**, 139 (1974); **4**, 149 (1974).

(39) A. Chutjian, S. K. Srivastava, S. Trajmar, and W. Williams, *J. Chem. Phys.*, **64**, 4791 (1976); J. Hayes, D. C. Cartwright, S. Trajmar, and A. Chutjian, in preparation.

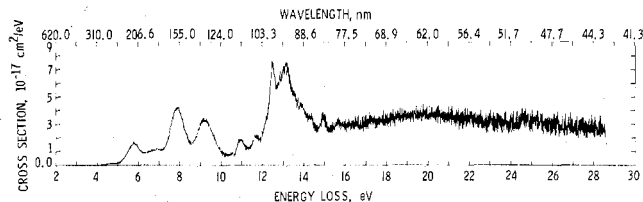


**Figure 10.** Optical absorption spectrum of  $\text{UF}_6$  obtained by high-energy electron impact method.

optical absorption cross sections extending down to 435 Å (see Figure 10), which agrees well with optical results in the region of overlap.

A survey of oscillator strength measurements on various molecular species has been made by Lassette<sup>5</sup> and Celotta and Heubner.<sup>6</sup>

**Inner-Shell Excitations.** There has been a great deal of interest recently in electron impact excitation of inner shells of atoms and molecules.<sup>41-43</sup> In this area the electron impact technique has a number of definite advantages over optical methods. A 75-meV resolution at 400-eV energy loss, which is easily achieved in electron scattering, is equivalent to a band pass of 0.006 Å at 31 Å. It has been verified by King et al.<sup>41</sup> that photoabsorption spectra can be simulated by electron-energy-loss studies at high impact energies and at low scattering angles for inner-shell excitations in atoms. King et al.,<sup>44</sup> using 1.5-keV electrons, were able to resolve vibrational structure in the K-shell excitation of  $\text{N}_2$  corresponding to the promotion of a 1s electron to the first unfilled ( $\pi_g$  2p) orbital at around 400-eV energy loss. There are two interesting aspects of this excitation process: (a) the probability for this excitation is higher than the sum of probabilities for exciting all discrete peaks below the ionization threshold, (b) the removal of the 1s electron generates a hole which is localized (at least to some degree) on the nitrogen atom.<sup>43</sup> The other electrons of the molecule then move in a mean electrostatic potential similar to that of the outer electrons of the neutral NO molecule, which is called the "equivalent core molecule".<sup>45</sup> The observed vibrational spacings, therefore, correspond to those of the NO, not the  $\text{N}_2$  molecule. With the utilization of this effect, one can obtain information about molecular species which are not commonly available. For example, starting with  $\text{O}_2$  the equivalent core molecule will be OF.

**Spectroscopy of Negative Ions.** Resonance in electron-scattering processes and their associated angular distributions have been extensively studied and have yielded information about the energies and symmetry properties of negative atomic and molecular ion states.<sup>30,46,47</sup> The resonance energy deduced from the experiment gives the location of the negative ion state, and under favorable conditions, the angular distributions are uniquely determined by the symmetry of the initial, final, and resonant states of the target molecule. This distribution can, therefore, be predicted, and a

(40) S. K. Srivastava, D. C. Cartwright, S. Trajmar, A. Chutjian, and W. Williams, *J. Chem. Phys.*, **65**, 208 (1976).

(41) G. C. King, M. Tronc, F. H. Read, and R. C. Bradford, *J. Phys. B*, **10**, 2479.

(42) F. H. Read, *J. Phys. (Paris)*, **39**, 82 (1978).

(43) M. Tronc, G. C. King, and F. H. Read, *J. Phys. B*, **12**, 132 (1979).

(44) G. C. King, F. H. Read, and M. Tronc, *Chem. Phys. Lett.*, **52** 50 (1977).

(45) G. R. Wight, C. E. Brion, and M. J. Van der Wiel, *J. Electron Spectrosc. Relat. Phenom.*, **1**, 457 (1972/73).

(46) G. J. Schulz, *Rev. Mod. Phys.*, **45**, 378 (1973).

(47) D. E. Golden, *Adv. At. Mol. Phys.*, **14**, 1 (1978).

comparison of the predicted and measured angular distributions can then identify the symmetry of the intermediate state. (See, e.g., ref 48-50).

As an example let us consider the shape resonance which occurs in e-H<sub>2</sub> collisions at around 3 eV. The symmetry of this resonance has been predicted to be  $^2\Sigma_u^+$ ,<sup>51</sup> and the angular distribution associated with this symmetry is:  $\sigma(\theta) \propto 1 + 2 \cos^2 \theta$ . This prediction has been confirmed by the measurement of the angular distribution of the scattered electrons in the vibrational excitation channel.<sup>52</sup>

Very recently Langendam et al.<sup>53</sup> and Langendam and Van der Wiel<sup>54</sup> investigated the energy level structure of Ne<sup>-</sup> by a very elegant free-free absorption experiment. In this experiment the incident electron (with the proper energy) is temporarily ( $\sim 10^{-13}$  s) trapped by neon. In the second step a laser-induced transition takes place to a higher negative ion state. In subsequent steps the excited Ne<sup>-</sup> autoionizes to produce excited neutral Ne, which in turn decays by UV photon emission. By tuning the laser wavelength and detecting the UV photon emission, one can utilize the two-state resonance enhancements and the high-resolution capability of the laser to do spectroscopy on a short-lived negative ion.

(48) J. N. Bardsley and F. H. Read, *Chem. Phys. Lett.*, **2**, 333 (1968).

(49) E. S. Chang, *J. Phys. B*, **10**, L677 (1977).

(50) J. X. H. Brunt, G. C. King, and F. H. Read, *J. Phys. B*, **11**, 173 (1978).

(51) J. N. Bardsley, A. Herzenberg, and F. Mandl, *Proc. Phys. Soc. (London)*, **89**, 305 (1966).

(52) H. Ehrhardt, L. Langhaus, F. Linder, and H. S. Taylor, *Phys. Rev.*, **173**, 222 (1968).

(53) P. J. K. Langendam, M. Gavrila, J. P. J. Kaandorp, and M. J. Van der Wiel, *J. Phys. B*, **9**, L453 (1976).

(54) P. J. K. Langendam and M. J. Van der Wiel, *J. Phys. B*, **11**, 3603 (1978).

## Concluding Remarks

The range of electron impact spectroscopy has been indicated here through a few simple examples. The main advantages of electron impact spectroscopy are the elimination of optical selection rules in excitation processes and the ability to scan the spectrum from the infrared to the X-ray region with the same experimental setup. More detailed information about the excitation processes can be obtained by measurements in which the scattered electron is detected in coincidence with secondary particles (electrons, photons, ions). The discussion of these topics is, however, beyond the scope of the present Account.

The experimental techniques and calibration methods for generating accurate electron impact cross sections became available only very recently, and one can expect a large body of reliable cross section data in the coming years. The application of coincidence techniques will enable us to reveal the details of complex excitation, dissociation, and ionization processes and to investigate electron and nuclear spin effects, the degree of coherence in simultaneous excitation of overlapping states, etc. The application of lasers in connection with electron impact phenomena represents a virgin area where activities are just beginning. Finally, extension of the present day techniques to excited and ionic targets, to free radical species, to complex molecules, and to solid surfaces can be expected in the near future.

*I express my gratitude to my collaborators whose work is quoted in this article. This work was supported by the National Aeronautics and Space Administration through Contract NAS7-100 to the Jet Propulsion Laboratory, California Institute of Technology.*

# Molecular Multiphoton Ionization Spectroscopy

PHILIP M. JOHNSON

*Department of Chemistry, State University of New York, Stony Brook, New York 11794*

*Received June 20, 1979*

When very intense visible or ultraviolet light interacts with molecules a great many interesting things can occur which do not happen under normal illumination conditions. Multiphoton processes can occur in which several photons interact simultaneously with the molecule, in contrast to the normal situation of just a single photon being absorbed or emitted at a time. Improbable as these transitions may be, they can be used to raise a molecule into one of its excited electronic states if the photon flux is great enough. With currently available pulsed dye lasers not tuned to a direct absorption of a molecule, even though just one photon in

$10^{10}$  gets absorbed, there are so many photons in a pulse that one can excite every molecule in a focal region. The electronically excited molecule is still bathed in a very intense field of radiation and can absorb additional photons until it is removed from a resonant condition by ionization, dissociation, reemission of photons, or the end of the light pulse. The means by which a molecule loses its excess energy, be it by ionization, emission of a photon, decomposition, or radiationless transition, can be used to detect the existence of that electronic state and thus be used as a means of knowing when a multiphoton transition has taken place. And the wavelength dependence of multiphoton transitions reveals much about the electronic structure of the molecule. For many excited electronic states their most probable fate in an intense light field is ionization, and I will discuss the use of multiphoton ionization (MPI) as a technique for the elucidation of excited-state structure,

Philip Johnson (born in Vancouver, WA, in 1940) received a B.S. from the University of Washington and his Ph.D. degree from Cornell University. After postdoctoral work at the University of Chicago he took a position in the Department of Chemistry of the State University of New York at Stony Brook, where he is now a professor. His research interests include the investigation of molecular electronic structure and the development of new techniques for the examination of the properties and dynamics of excited electronic states.